The Astrophysical Journal Supplement Series, 181:53–61, 2009 March doi:10.1088/0067-0049/181/1/53

INFRARED SPECTRA OF AMMONIA–WATER ICES

Weijun Zheng[1,2,3], David Jewitt[1,4], and Ralf I. Kaiser[2,4]
[1] Institute for Astronomy, University of Hawaii, Honolulu, HI 96822, USA; jewitt@ifa.hawaii.edu
[2] Department of Chemistry, University of Hawaii, Honolulu, HI 96822, USA; ralfk@hawaii.edu
[3] Beijing National Laboratory for Molecular Sciences, State Key Laboratory of Molecular Reaction Dynamics, Institute of Chemistry, Chinese Academy of Sciences, Beijing 100190, P. R. of China; zhengwj@iccas.ac.cn
Received 2007 October 28; accepted 2008 September 30; published 2009 February 19

ABSTRACT

We conducted a systematic study of the near-IR and mid-IR spectra of ammonia–water ices at various NH_3/H_2O ratios. The differences between the spectra of amorphous and crystalline ammonia–water ices were also investigated. The 2.0 μm ammonia band central wavelength is a function of the ammonia/water ratio. It shifts from 2.006 ± 0.003 μm (4985 ± 5 cm^{-1}) to 1.993 ± 0.003 μm (5018 ± 5 cm^{-1}) as the percentage of ammonia decreases from 100% to 1%. The 2.2 μm ammonia band center shifts from 2.229 ± 0.003 μm (4486 ± 5 cm^{-1}) to 2.208 ± 0.003 μm (4528 ± 5 cm^{-1}) over the same range. Temperature-dependent shifts of those bands are below the uncertainty of the measurement, and therefore are not detectable. These results are important for comparison with astronomical observations as well as for estimating the concentration of ammonia in outer solar system ices.

Key words: infrared: general – methods: laboratory – planets and satellites: general

Online-only material: color figures

1. INTRODUCTION

Nitrogen is one of the most cosmically abundant elements (7×10^{-5} relative to hydrogen by number; Snow & Witt 1996) and its main hydride, ammonia, is potentially a major carrier of this element. The abundance of ammonia ice in dust grains in cold molecular clouds has been suggested to be 1–10% with respect to water (Gibb et al. 2004; Greenberg et al. 1983), while in the cold dust envelopes of young stellar objects, the ammonia ice fraction is 5% or less (Dartois & d'Hendecourt 2001). Ammonia is a potentially important chemical component in the solar system both as a repository of nitrogen in primitive objects such as the nuclei of comets and as an agent by which ice convection can be enhanced in the deep interiors of ice-rich bodies. It has been found in the atmospheres of Jupiter (Atreya et al. 2003), Saturn (Atreya et al. 2003), Uranus (Hofstadter & Muhleman 1989), and Neptune (Lindal 1992). In comets, ammonia is present at the 1% level relative to water ice (Bockelee-Morvan et al. 2004).

Solid ammonia and its hydrates have two major IR bands in the near-IR (NIR) region, one centered at ∼2.2 μm (4545 cm^{-1}) and the other centered at ∼2.0 μm (5000 cm^{-1}). The 2.0 μm band has not yet been reliably identified in astronomical spectra, perhaps in part due to the overlap of the weak ammonia 2.0 μm band with the much stronger water band at the same wavelength and/or due to radiative transfer effects inside a granular regolith. Instead, claimed detections of ammonia–water ice are based upon the 2.2 μm band, which falls in a relatively "clean" portion of the spectrum, outside the water ice 2.0 μm band. Furthermore, it is difficult to estimate the concentration of ammonia where it is detected, due to the paucity of relevant, reliable laboratory data. Despite these difficulties, ammonia or ammonia hydrate has been reported to be present on the surfaces of various icy bodies, such as Saturn's satellite Enceladus (Emery et al. 2005; Verbiscer et al. 2006), Uranus's satellite Miranda (Bauer et al. 2002), Pluto's satellite Charon (Brown & Calvin 2000; Dumas et al. 2001; Cook et al. 2007), and Kuiper Belt Object (50000) Quaoar (Jewitt & Luu 2004; Schaller & Brown 2007). As noted, the implied abundances are highly uncertain but values of order 1% have been reported, consistent with the cometary value. In fact, ammonia is expected to be selectively depleted relative to water when exposed to energetic particles from the solar wind and to cosmic rays (Lanzerotti et al. 1984; Moore et al. 2007). In this sense, the very existence of ammonia ice or hydrate on an exposed surface may suggest the action of resurfacing processes on distant small bodies of the Solar system.

In the interiors of icy bodies, ammonia may play an especially important role in reducing the melting point relative to pure water ice, and hence in promoting geophysical heat loss through convection (Kargel & Pozio 1996; Multhaup & Spohn 2007; Spohn & Schubert 2003). In this way, ammonia may promote the geological resurfacing of icy bodies in the middle and outer solar system (e.g., Mitri et al. 2008). Mild heating of radiolytically processed ammonia ice has been proposed as a possible driver of outgassing activity observed on Saturn's satellite Enceladus (Loeffler et al. 2006). While by no means providing a unique explanation of Enceladus' behavior, this suggestion does point to the important and unexpected roles that might be played by ammonia.

Although some laboratory NIR spectra of ammonia–water ice have been reported previously (Brown et al. 1988; Dalton et al. 2001; Schmitt et al. 1998), only the recent spectroscopic study of ammonia–water ice in the laboratory by Moore et al. (2007) presented the IR spectra of ammonia–water ice at different NH_3/H_2O ratios, focusing on the bands at 2.0 μm and 2.2 μm. Most spectra reported by Moore et al. are measured in the amorphous phase. Our work is independent of, and complementary to, that by Moore et al. In addition to the 2.0 μm and 2.2 μm bands, we also measure the astronomically important 1.5 μm band where the amorphous and crystalline ice spectra of water are most distinct. Most of the water ice (containing ammonia or not) in the outer solar system is found to be crystalline ice based on the water 1.5 μm and 1.65 μm bands (e.g., Jewitt & Luu 2004; Cook et al. 2007; Trujillo et al. 2007). Therefore, it is

[4] Authors to whom any correspondence should be addressed.

important to conduct more systematic studies on the IR spectra of ammonia–water ice in crystalline phase in a range that covers both the 1.5 μm water band and 2.2 μm ammonia band.

2. EXPERIMENTAL DETAILS

The experiments were carried out in an ultra-high vacuum chamber with 7×10^{-11} torr background pressure (Zheng et al. 2006). A two-stage, closed-cycle helium refrigerator coupled with a rotary platform is attached to the main chamber and holds a polished polycrystalline silver mirror serving as a substrate for the ice condensation. With the combination of the closed-cycle helium refrigerator and a programmable temperature controller, the temperature of the silver mirror can be regulated precisely to ± 0.3 K between 10 K and 350 K. The IR spectra of the samples were measured by a Fourier Transform IR Spectrometer (Nicolet 6700 FTIR). The species released into the gas phase were monitored with a quadrupole mass spectrometer (Balzer QMG 420).

The ammonia–water ice mixtures were prepared by condensing anhydrous ammonia (99.99%; Matheson Gas Products, Inc.) and water vapor onto the silver substrate at 10 K. The ammonia and water were introduced into the chamber simultaneously through separate capillaries (one for ammonia, the other for water). The angle between the capillaries was about 55°, while the normal to the substrate bisected that angle. The capillaries were located 4 cm away from the silver substrate. During the condensation, the total pressure of ammonia and water in the main chamber was maintained at approximately 2.2×10^{-8} torr for about 20 minutes. The partial pressures of ammonia and water were varied in order to produce ice mixtures with different NH_3/H_2O ratios. For example, in order to produce a 1:9 NH_3:H_2O ice mixture, the partial pressure of ammonia was controlled at 2.4×10^{-9} torr and that of water at 2.0×10^{-8} torr. We used nominal gas correction factors (H_2O: 1.12; NH_3: 1.23) to calculate the actual partial pressures of water and ammonia based on the numbers measured by the ionization gauge because the ionization gauge responds to water and ammonia differently.

In this experiment, we used the Lambert–Beer law to estimate the sample thickness. The column density of pure water ice without ammonia was estimated to be about 2.7×10^{17} molecule cm^{-2} based on the integrated IR absorption coefficient of the 3 μm feature of water (2×10^{-16} cm molecule^{-1}; Gerakines et al. 1995). A separate estimate of 8.5×10^{17} molecule cm^{-2} was obtained from the integral absorption coefficient of the 2 μm feature of water ice (1.2×10^{-18} cm molecule^{-1}; Gerakines et al. 2005). The column density of pure ammonia ice was about 1.9×10^{17} molecule cm^{-2} from the integrated IR absorption coefficient of the ν_2 band of NH_3 (1.7×10^{-17} cm molecule^{-1}; Dhendecourt & Allamandola 1986). Based on the column densities, we estimated the thicknesses of our samples to be between 80 nm and 270 nm. The relative variations of the thickness in our experiments were less than 5% from day to day although the absolute ice thickness has a large uncertainty. We note that Teolis et al. (2007) criticized our method of measuring sample thickness, but used column densities 2×10^{18}, 6×10^{18}, 8×10^{18} molecule cm^{-2} or higher, whereas we used only 10^{17} molecule cm^{-2}. Our sample thickness is much thinner than theirs and, therefore, errors caused by interference effects can be ignored in our experiments. Mastrapa & Brown (2006) estimated their sample thickness by counting the interference fringes of an He–Ne laser beam passed their sample. Their method should be good for measuring sample thicknesses much greater than the laser wavelength, but is unsuited to the thin samples used here.

3. RESULTS AND DISCUSSION

Figure 1 shows the IR spectra of water–ammonia ice mixtures containing 1%, 2.5%, 5%, and 10% ammonia. The samples were condensed at 10 K, heated to 130 K, held at 130 K for 3 hr for crystallization and then re-cooled to the corresponding temperatures. It has been reported that pure ammonia begins to sublimate measurably at about 80 K (Zheng & Kaiser 2007). We monitored the species (i.e., NH_3, H_2O, etc.) released into the gas with a quadrupole mass spectrometer. The intensity of the mass spectral signal indicates that ammonia loss during the heating can be ignored, probably because the ammonia molecules are trapped in the water ice. The 1.5 μm band and the 3 μm band are similar to those of pure water ice. The 2.0 μm and 2.2 μm ammonia bands are centered at 5018 ± 5 cm^{-1} (1.993 μm) and 4528 ± 5 cm^{-1} (2.208 μm), respectively. These two bands can be attributed to the ammonia ($\nu_3 + \nu_4$) and ($\nu_3 + \nu_2$) combination modes (Ferraro et al. 1980; Zheng & Kaiser 2007). We find that the temperature shift of ammonia bands is below the uncertainty of the measurement in the temperature range 10–130 K. Our laboratory results show that the 2.0 μm band of ammonia is still visible in the ice with 1% ammonia. This result is in agreement with Moore et al. (2007).

Since the ices in the outer solar system contain much more water than ammonia, the ammonia–water ice mixtures with 1%, 2.5%, 5%, and 10% ammonia are the most relevant for application to the outer solar system. For completeness, we also show the spectra of water–ammonia ice mixtures containing 50%, 90%, 95%, and 99% ammonia (Figure 2). These samples were condensed at 10 K, heated to 84 K, held at 84 K for 3 hr, and re-cooled to the corresponding temperatures. Our mass spectral results show that the sublimation of ammonia at temperature higher than 85 K cannot be ignored. Therefore, these samples were heated to only 84 K. As shown in Figure 2, for the 99% ammonia ice, there is an absorption feature at 2.30 μm (4345 cm^{-1}) which can be assigned to the ($\nu_1 + \nu_2$) combination mode of ammonia (Ferraro et al. 1980; Zheng & Kaiser 2007). The intensity of the 2.30 μm feature decreases with increasing percentage of water in the sample.

Figures 3 and 4 compare the spectra of the amorphous (blue) and crystalline (red) phases. The crystalline spectra (Figure 3(A1)–(D1)) clearly show the 1.65 μm water band that does not exist in the amorphous spectra. In Figure 3(A2)–(D2), the mid-IR spectra of ammonia–water ice with ammonia $\leqslant$10% are very similar to that of pure water ice except for a peak of ammonia ν_2 mode at $\sim$1122 cm^{-1} (8.913 μm) and a shoulder at 2700–3000 cm^{-1} (3.704–3.333 μm) which probably is due to the formation of ammonia hydrate. The ammonia ν_4 is observed at 1630 cm^{-1} (6.135 μm) in the crystalline spectra. The 3 μm band shows more fine structure in the crystalline spectra than in the amorphous spectra (Figure 3(A2)–(D2)). Similarly, in Figure 4, the spectra of the crystalline samples show more fine structure than those of the amorphous samples.

The positions of the 2.0 μm and 2.2 μm ammonia bands are listed in Table 1. Figure 5 shows the wavelength shift of the 2.0 μm and 2.2 μm ammonia bands with the change in composition of ammonia–water crystalline ice. The wavelengths, measured from the maxima of the ammonia bands, shift toward shorter wavelengths as the water/ammonia percentage increases in the ice. The 2.0 μm ammonia band shifts from 2.006 ± 0.003 μm (4985 ± 5 cm^{-1}) to 1.993 ± 0.003 μm (5018 ± 5 cm^{-1}) as the percentage of ammonia decreases from 100% to 1%. The 2.2 μm ammonia band shifts from

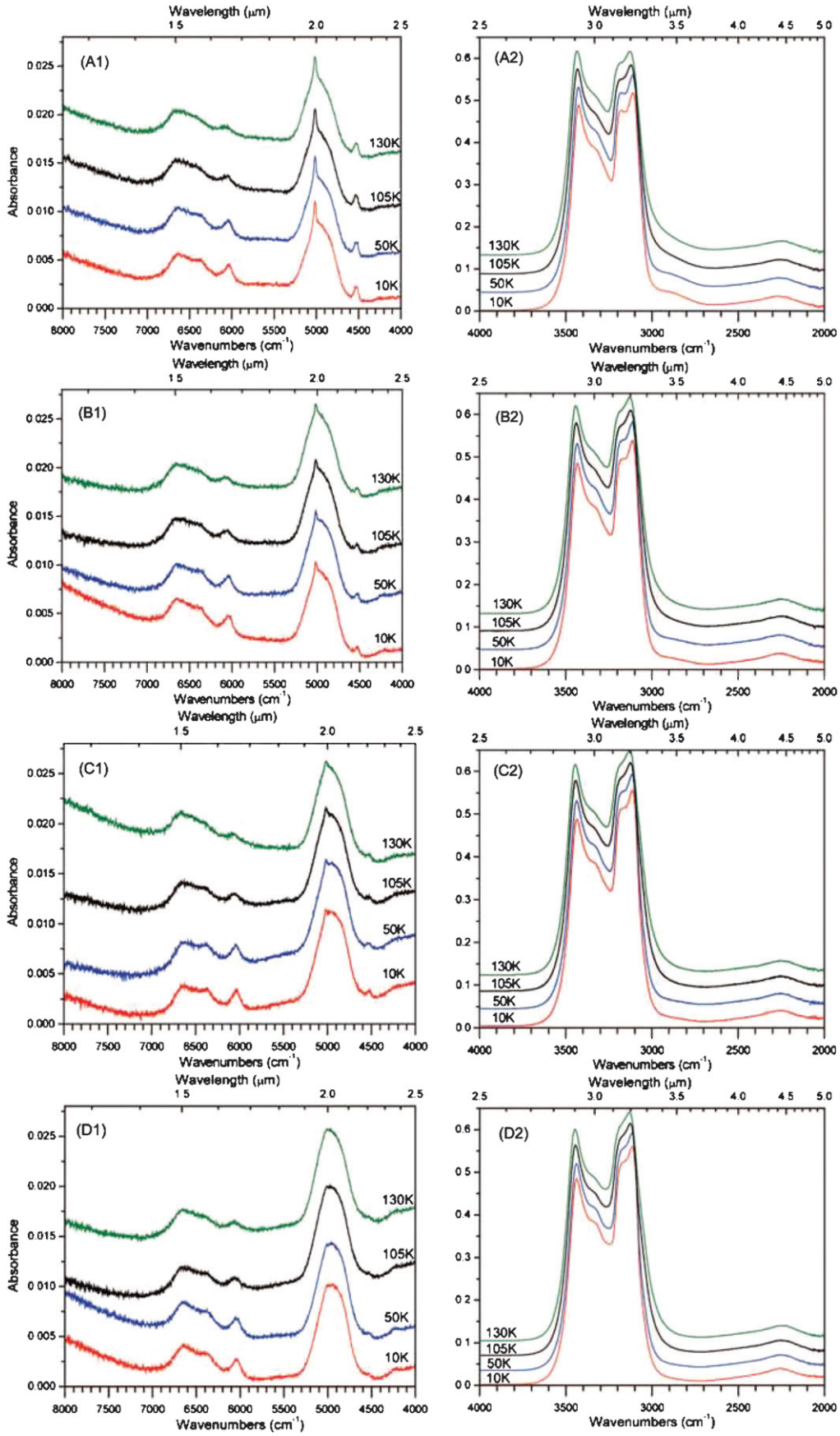

Figure 1. IR spectra (8000–2000 cm^{-1}) of water–ammonia ice mixture with 10%, 5%, 2.5%, and 1% ammonia. The samples were condensed at 10 K, heated to 130 K, stayed at 130 K for 3 hr, then cooled down to the corresponding temperatures. (A1) and (A2) 10%; (B1) and (B2) 5%; (C1) and (C2) 2.5%; (D1) and (D2) 1%. (A color version of this figure is available in the online journal.)

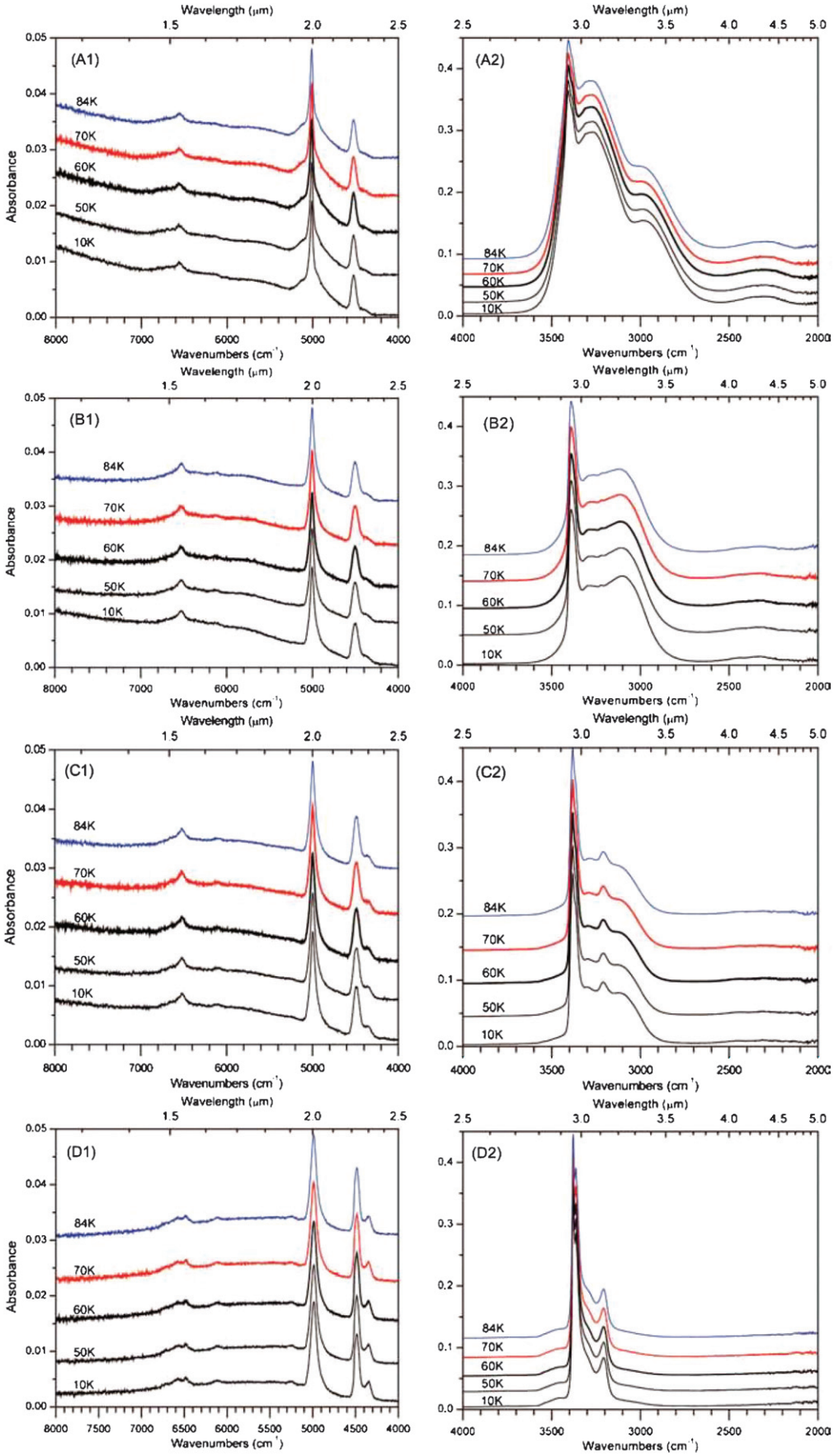

Figure 2. IR spectra (8000–2000 cm^{-1}) of water–ammonia ice mixture with 50%, 90%, 95%, and 99% ammonia. The samples were condensed at 10 K, heated to 84 K, stayed at 84 K for 3 hr, then cooled down to the corresponding temperatures. (A1) and (A2) 50%; (B1) and (B2) 90%; (C1) and (C2) 95%; (D1) and (D2) 99%. (A color version of this figure is available in the online journal.)

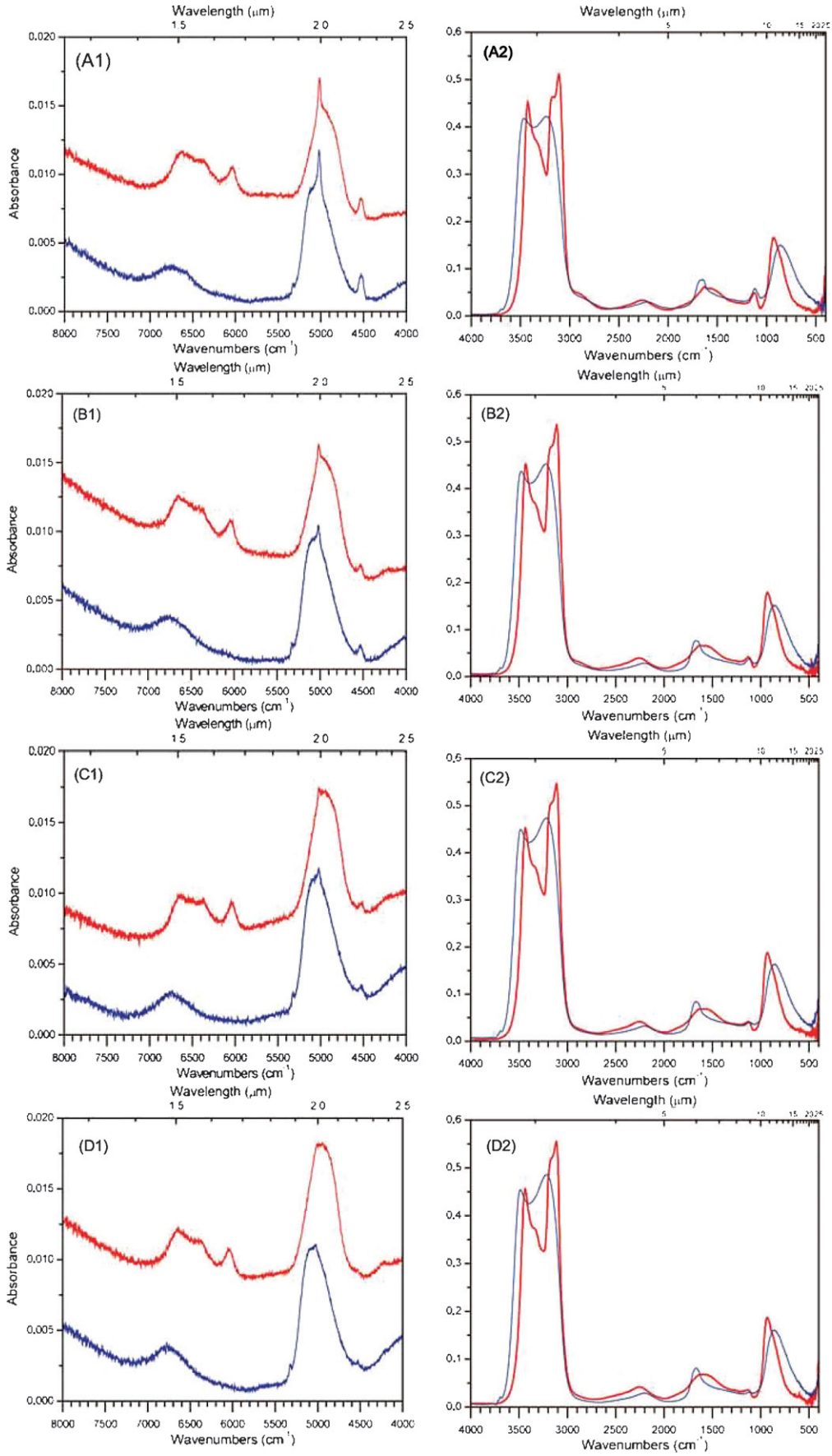

Figure 3. NIR and mid-IR spectra of water–ammonia ice 10%, 5%, 2.5%, and 1% ammonia at 10 K. A comparison between the amorphous sample (blue) and crystalline sample (red). The crystalline samples had been heated to 130 K and re-cooled to 10 K. (A1) and (A2) 10%; (B1) and (B2) 5%; (C1) and (C2) 2.5%; (D1) and (D2) 1%.

(A color version of this figure is available in the online journal.)

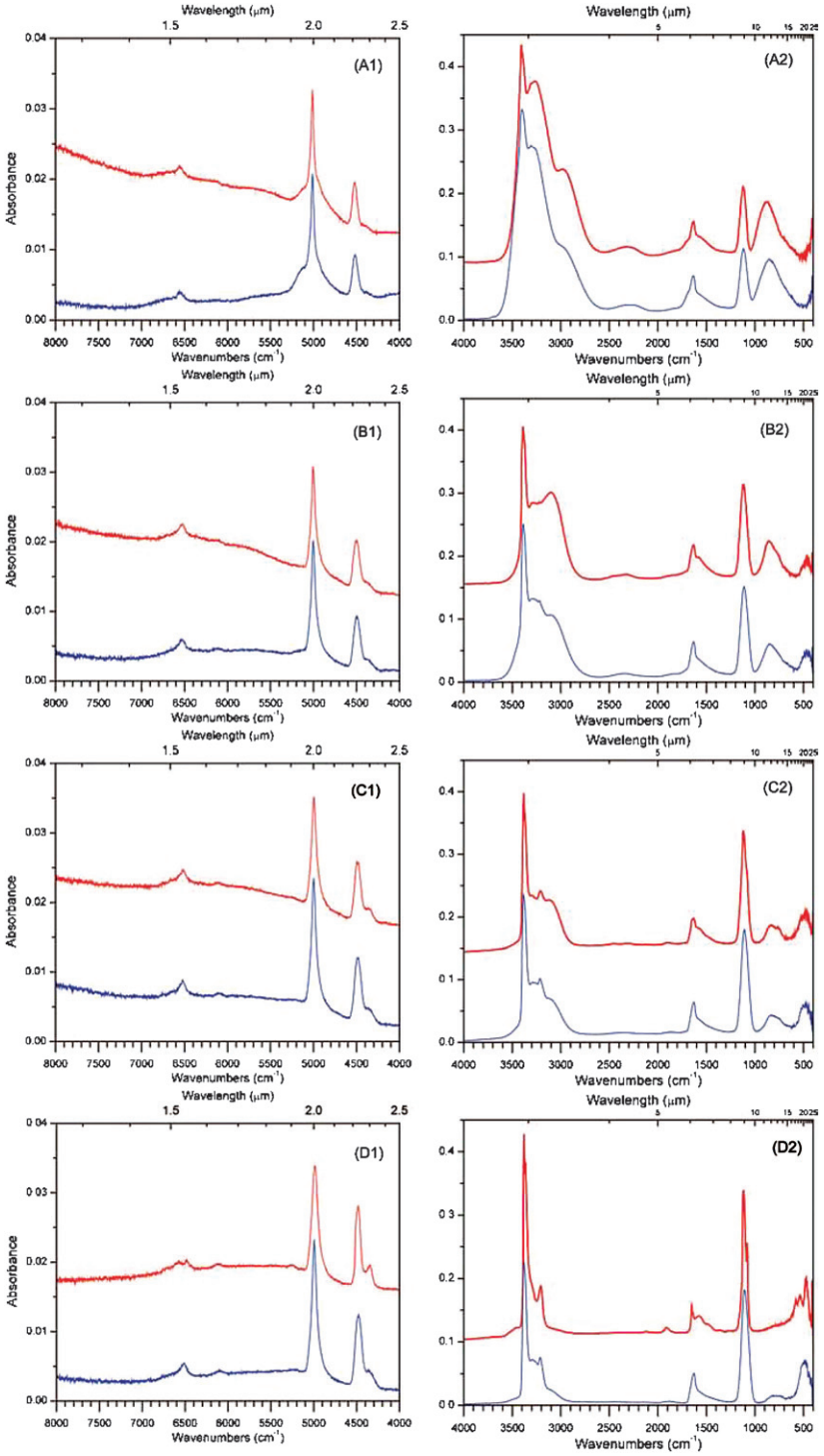

Figure 4. NIR and mid-IR spectra of water–ammonia ice 50%, 90%, 95%, and 99% ammonia at 10 K. A comparison between the amorphous sample (blue) and crystalline sample (red). The crystalline samples had been heated to 84 K and re-cooled to 10 K. (A1) and (A2) 50%; (B1) and (B2) 90%; (C1) and (C2) 95%; (D1) and (D2) 99%.

(A color version of this figure is available in the online journal.)

2.229 ± 0.003 μm (4486 ± 5 cm^{-1}) to 2.208 ± 0.003 μm (4528 ± 5 cm^{-1}) when the percentage of ammonia decreases from 100% to 1%. For comparison, the measured wavelengths of the purported ammonia-related absorption in the spectrum of Pluto's satellite Charon are 2.1995 ± 0.0015 μm and 2.2131 ± 0.0007 μm on the Pluto-facing and anti-Pluto hemispheres, respectively (Cook et al. 2007). While a detailed interpretation would require modeling of radiative transfer in the fragmented regolith of Charon, it is clear that the central wavelengths imply a rather modest ammonia/water ratio in the ice, on the order of 1%. A possibly related band has been reported in Kuiper Belt Object (50000) Quaoar, with a center measured at 2.220 ± 0.005 μm (Jewitt & Luu 2004) and 2.205 ± 0.002 μm (Schaller & Brown 2007). These wavelengths are again consistent with

Table 1
Positions of the 2.0 and 2.2 μm Ammonia Bands for Ammonia–Water Crystalline Ice with Different Ratios

Percentage of NH_3 (%)	Percentage of H_2O (%)	2.0 μm Band (μm)	2.2 μm Band (μm)
100	0	2.006 (4985 cm^{-1})	2.229 (4486 cm^{-1})
99	1	2.004 (4989 cm^{-1})	2.229 (4486 cm^{-1})
95	5	2.001 (4998 cm^{-1})	2.229 (4486 cm^{-1})
90	10	1.998 (5004 cm^{-1})	2.222 (4501 cm^{-1})
50	50	1.995 (5012 cm^{-1})	2.211 (4522 cm^{-1})
10	90	1.993 (5017 cm^{-1})	2.208 (4528 cm^{-1})
5	95	1.993 (5018 cm^{-1})	2.208 (4528 cm^{-1})
2.5	97.5	1.992 (5020 cm^{-1})	2.208 (4528 cm^{-1})
1	99	1.992 (5020 cm^{-1})	2.208 (4528 cm^{-1})

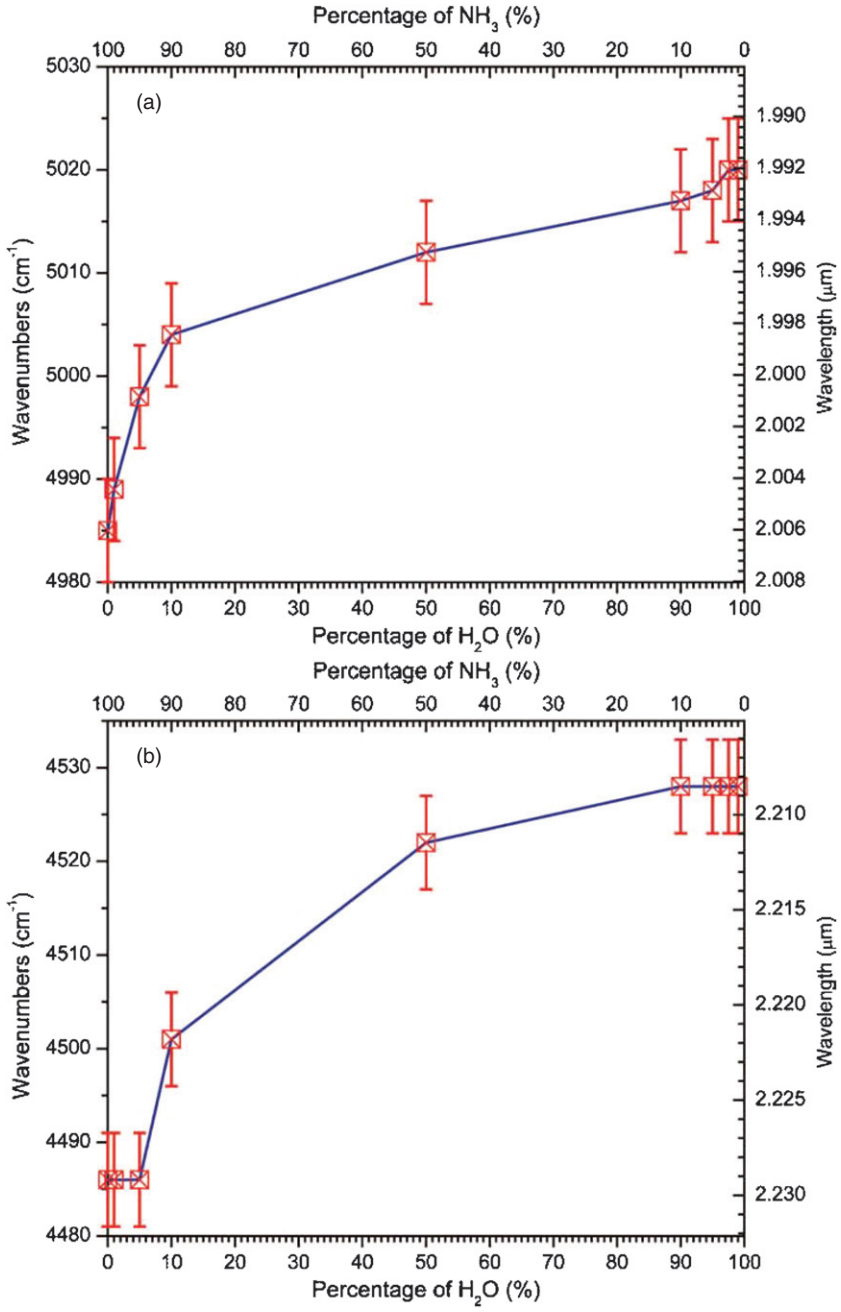

Figure 5. Shift of the ammonia 2.0 μm and 2.2 μm bands due to the addition of water into the ice mixture. (a) 2.0 μm band and (b) 2.2 μm band.
(A color version of this figure is available in the online journal.)

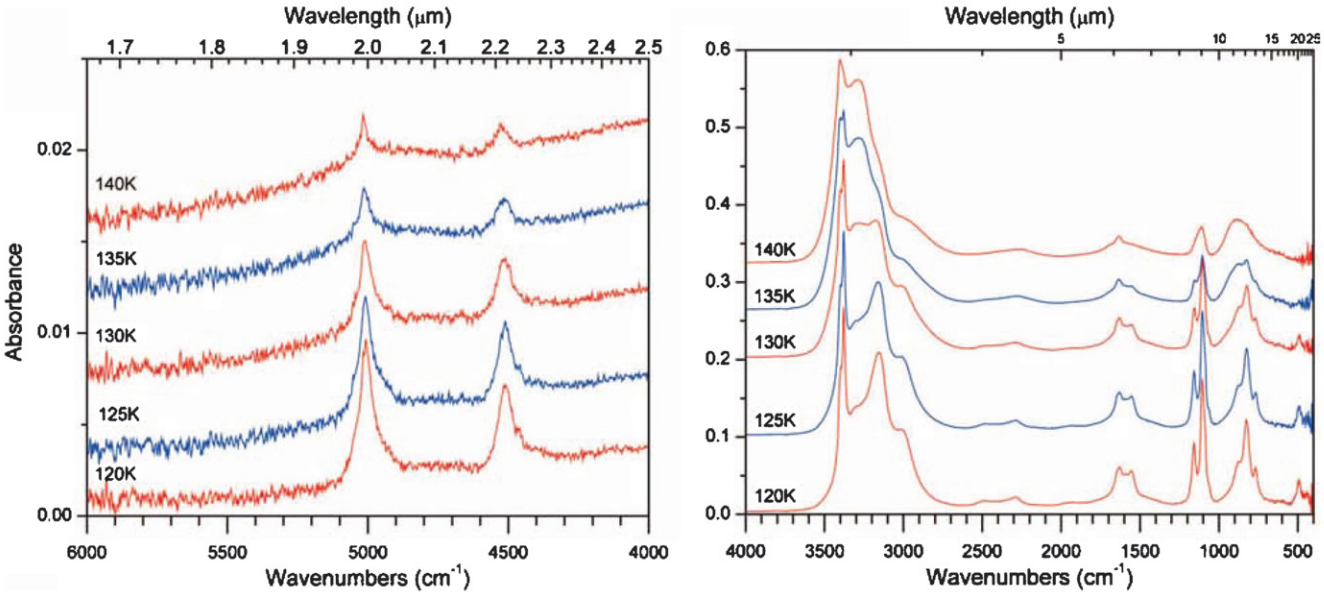

Figure 6. IR spectra of 9:1 NH_3/H_2O ice after the ammonia loss. The spectra were obtained by warming the ammonia–water ice of 90% ammonia to the specific temperatures. The spectra at 120 K and 125 K are similar to the spectrum of $2NH_3{\cdot}H_2O$.

(A color version of this figure is available in the online journal.)

the presence of an ammonia–ice mixture, but the latter authors report additional bands at 2.32 μm and 2.38 μm that suggest an origin for the 2.22 μm band partly or wholly in methane ice.

The spectra of $2NH_3{\cdot}H_2O$ and $NH_3{\cdot}H_2O$ have been reported by Bertie & Devlin (1984), Bertie & Morrison (1980) and Moore et al. (2007). Bertie & Shehata (1984) have also measured the IR spectrum of $NH_3{\cdot}2H_2O$. We could reproduce their $2NH_3{\cdot}H_2O$ spectrum by heating up the ammonia–water mixture with 90% ammonia to 120 K to reduce the percentage of ammonia. Figure 6 shows the IR spectra at different temperatures. The spectra at 120 K and 125 K are very similar to the $2NH_3{\cdot}H_2O$ spectra of Bertie & Devlin (1984), Bertie & Morrison (1980) and Moore et al. (2007). Further heating up can produce the spectrum of lower NH_3/H_2O ratio, for example, the spectra between 130 and 140 K are somewhat similar to the $NH_3{\cdot}H_2O$ spectra reported by Bertie & Devlin and Moore et al., but they are not exactly the same. The 140 K spectrum in Figure 6 is more similar to our own spectra of 1:1 NH_3/H_2O ratio (Figure 4(A2)). The spectra of ammonia–water ice mixtures with 1%–10% ammonia are very different from those of ammonia hemihydrate ($2NH_3{\cdot}H_2O$), ammonia monohydrate ($NH_3{\cdot}H_2O$), or ammonia dihydrate ($NH_3{\cdot}2H_2O$). Thus, we are unable to tell whether these mixtures are in $NH_3{\cdot}H_2O$ form or $NH_3{\cdot}2H_2O$ form. Since the percentage of water in these mixtures is much greater than that of ammonia, it might be possible that each ammonia molecule interacts with more than two water molecules.

In order to make it convenient for the readers to compare the spectra of ammonia–water ice at different ratios and for astronomers to estimate the concentrations of ammonia on space objects based on our spectra, we summarize the IR absorption spectra of the ammonia–water ice mixtures in Figures 7 and 8.

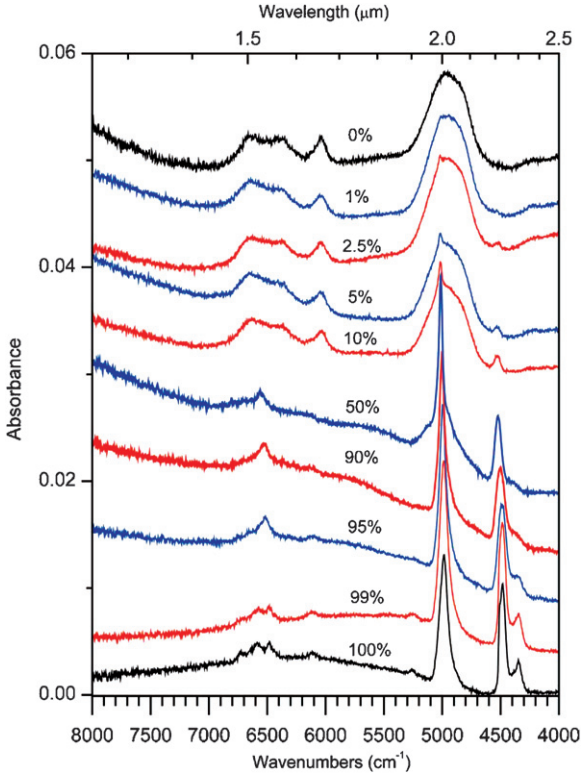

Figure 7. NIR spectra of water–ammonia ice mixtures of different ratios. The spectra were taken at 10 K. The spectra with 10%, 5%, 2.5%, and 1% ammonia had been annealed to 130 K. Those with 50%, 90%, 95%, and 99% ammonia had been annealed to 84 K.

(A color version of this figure is available in the online journal.)

4. SUMMARY

We present the first experiments conducted under ultra-high vacuum conditions on the NIR and mid-IR spectra of water–ammonia mixtures, with the following astronomically relevant findings.

1. The 2.0 μm ammonia band shifts from 2.006 ± 0.003 μm (4985 ± 5 cm^{-1}) to 1.993 ± 0.003 μm (5018 ± 5 cm^{-1}) as the percentage of ammonia decreases from 100% to 1%. The 2.2 μm ammonia band shifts from 2.229 ± 0.003 μm (4486 ± 5 cm^{-1}) to 2.208 ± 0.003 μm (4528 ± 5 cm^{-1})

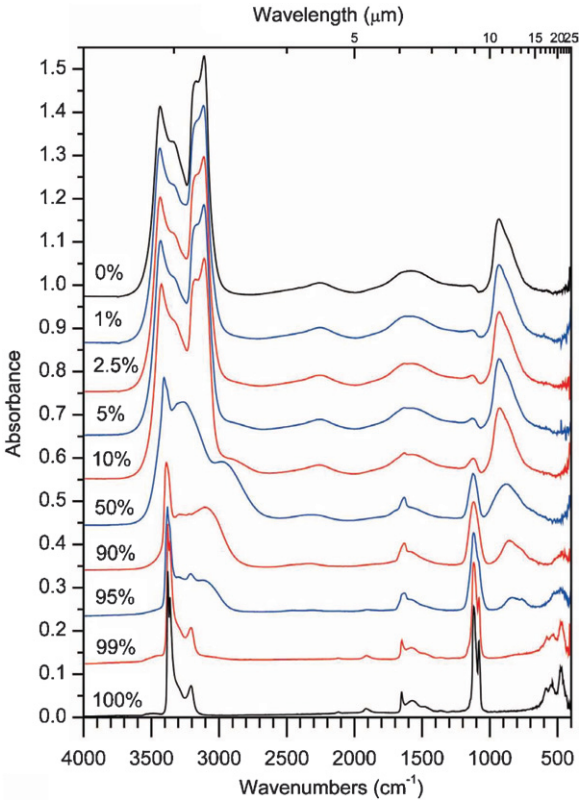

Figure 8. Mid-IR spectra of water–ammonia ice mixtures of different ratios. The spectra were taken at 10 K. The spectra with 10%, 5%, 2.5%, and 1% ammonia had been annealed to 130 K. Those with 50%, 90%, 95%, and 99% ammonia had been annealed to 84 K.

(A color version of this figure is available in the online journal.)

over the same range. The band centers do not measurably shift with temperature.

2. The 2.0 μm ammonia band remains visible even as the percentage of ammonia in the ice decreases to 1%. Curiously, there is no reported detection of this 2.0 μm ammonia band on outer solar system surfaces even though the 2.2 μm ammonia band has been frequently reported. The reason for this anomaly is not known.
3. The spectra of ammonia–water ice mixtures with 1%–10% ammonia are different from those of ammonia hemihydrate ($2NH_3 \cdot H_2O$), ammonia monohydrate ($NH_3 \cdot H_2O$), or ammonia dihydrate ($NH_3 \cdot 2H_2O$). One cannot simply assign the absorption features to these ammonia hydrates.
4. The spectra obtained in our experiments might be useful for comparison with astronomical observations to estimate the concentration of ammonia in outer solar system ices.

This work was financed by the US National Science Foundation (NSF; AST-0507763; D.J, R.I.K) and by the NASA Astrobiology Institute under Cooperative Agreement NNA04CC08A at the University of Hawaii-Manoa (W.Z). We are grateful to Ed Kawamura (Department of Chemistry, University of Hawaii at Manoa) for his electrical work.

REFERENCES

Atreya, S. K., Mahaffy, P. R., Niemann, H. B., Wong, M. H., & Owen, T. C. 2003, Planet. Space Sci., 51, 105
Bauer, J. M., et al. 2002, Icarus, 158, 178
Bertie, J. E., & Devlin, J. P. 1984, J. Chem. Phys., 81, 1559
Bertie, J. E., & Morrison, M. M. 1980, J. Chem. Phys., 73, 4832
Bertie, J. E., & Shehata, M. R. 1984, J. Chem. Phys., 81, 27
Bockelee-Morvan, D., Crovisier, J., Mumma, M., & Weaver, H. 2004, in Comets II, ed. M. Festou, H. Keller, & H. Weaver (Tucson, AZ: Univ. Arizona Press) 391
Brown, M. E., & Calvin, W. M. 2000, Science, 287, 107
Brown, R. H., Cruikshank, D. P., Tokunaga, A. T., Smith, R. G., & Clark, R. N. 1988, Icarus, 74, 262
Cook, J. C., Desch, S., Roush, T., Trujillo, C., & Geballe, T. 2007, ApJ, 663, 1406
Dalton, J. B., III, Curchin, J. M., & Clark, R. N. 2001, in Lunar and Planetary Institute Conference Abstracts, Temperature Dependence of Cryogenic Ammonia–Water Ice Mixtures and Implications for Icy Satellite Surfaces (Houston, TX: Lunar and Planetary Institute), 1496
Dartois, E., & d'Hendecourt, L. 2001, A&A, 365, 144
Dhendecourt, L. B., & Allamandola, L. J. 1986, A&AS, 64, 453
Dumas, C., Terrile, R. J., Brown, R. H., Schneider, G., & Smith, B. A. 2001, AJ, 121, 1163
Emery, J. P., Burr, D. M., Cruikshank, D. P., Brown, R. H., & Dalton, J. B. 2005, A&A, 435, 353
Ferraro, J. R., Sill, G., & Fink, U. 1980, Appl. Spectrosc., 34, 525
Gerakines, P. A., Bray, J. J., Davis, A., & Richey, C. R. 2005, ApJ, 620, 1140
Gerakines, P. A., Schutte, W. A., Greenberg, J. M., & Vandishoeck, E. F. 1995, A&A, 296, 810
Gibb, E. L., Whittet, D. C. B., Boogert, A. C. A., & Tielens, A. G. G. 2004, ApJS, 151, 35
Greenberg, J. M., van de Bult, C. E. P. M., & Allamandola, L. J. 1983, J. Phys. Chem., 87, 4243
Hofstadter, M. D., & Muhleman, D. O. 1989, Icarus, 81, 396
Jewitt, D. C., & Luu, J. 2004, Nature, 432, 731
Kargel, J. S., & Pozio, S. 1996, Icarus, 119, 385
Lanzerotti, L., Brown, W., Narcantonio, K., & Johnson, R. 1984, Nature, 312, 139
Lindal, G. F. 1992, AJ, 103, 967
Loeffler, M., Raut, U., & Baragiola, R. 2006, ApJ Lett., 649, 133
Mastrapa, R. M. E., & Brown, R. H. 2006, Icarus, 183, 207
Mitri, G., Showman, A., Lunine, J., & Lopes, R. 2008, Icarus, 196, 216
Moore, M. H., Ferrante, R. F., Hudson, R. L., & Stone, J. N. 2007, Icarus, 190, 260
Multhaup, K., & Spohn, T. 2007, Icarus, 186, 420
Schaller, E., & Brown, M. 2007, ApJ Lett., 670, 49
Schmitt, B., Quirico, E., Trotta, F., & Grundy, W. M. 1998, in ASSL Vol. 227: Solar System Ices, Optical Properties of Ices from UV to Infrared (Dordrecht: Kluwer), 199
Snow, T. P., & Witt, A. N. 1996, ApJ Lett., 468, 65
Spohn, T., & Schubert, G. 2003, Icarus, 161, 456
Teolis, B. D., Loeffler, M. J., Raut, U., Fama, M., & Baragiola, R. A. 2007, Icarus, 190, 274
Trujillo, C. A., Brown, M. E., Barkume, K. M., Schaller, E. L., & Rabinowitz, D. L. 2007, ApJ, 655, 1172
Verbiscer, A. J., et al. 2006, Icarus, 182, 211
Zheng, W., & Kaiser, R. I. 2007, Chem. Phys. Lett., 440, 229
Zheng, W. J., Jewitt, D., & Kaiser, R. I. 2006, AJ, 639, 534